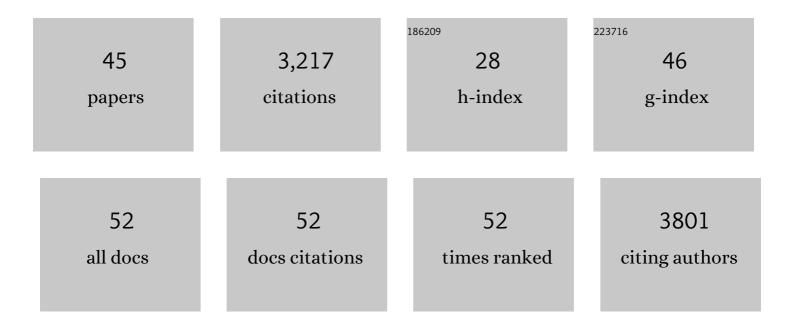
David D Hibbitts

List of Publications by Year in descending order

Source: https://exaly.com/author-pdf/1728111/publications.pdf Version: 2024-02-01



#	Article	IF	CITATIONS
1	Predicting diffusion barriers and diffusivities of C6–C12 methylbenzenes in MFI zeolites. Microporous and Mesoporous Materials, 2022, 333, 111705.	2.2	7
2	The Fischer-Tropsch synthesis: A few enduring mechanistic conundrums revisited. Journal of Catalysis, 2022, 405, 614-625.	3.1	7
3	Binding and Exchange Reactions of Hydrogen Isotopes on Surfaces of Dispersed Pt Nanoparticles. Journal of Physical Chemistry C, 2022, 126, 3923-3938.	1.5	3
4	Quantifying Effects of Active Site Proximity on Rates of Methanol Dehydration to Dimethyl Ether over Chabazite Zeolites through Microkinetic Modeling. ACS Materials Au, 2022, 2, 163-175.	2.6	7
5	Oxygen-Doped Carbon Supports Modulate the Hydrogenation Activity of Palladium Nanoparticles through Electronic Metal–Support Interactions. ACS Catalysis, 2022, 12, 7344-7356.	5.5	22
6	Hydrogenation and C S bond activation pathways in thiophene and tetrahydrothiophene reactions on sulfur-passivated surfaces of Ru, Pt, and Re nanoparticles. Applied Catalysis B: Environmental, 2021, 291, 119797.	10.8	9
7	Comparing alkene-mediated and formaldehyde-mediated diene formation routes in methanol-to-olefins catalysis in MFI and CHA. Journal of Catalysis, 2021, 400, 124-139.	3.1	12
8	Theoretical and Experimental Characterization of Adsorbed CO and NO on γ-Al ₂ O ₃ -Supported Rh Nanoparticles. Journal of Physical Chemistry C, 2021, 125, 19733-19755.	1.5	9
9	Experimental and Theoretical Assessments of Aluminum Proximity in MFI Zeolites and Its Alteration by Organic and Inorganic Structure-Directing Agents. Chemistry of Materials, 2020, 32, 9277-9298.	3.2	55
10	Rigid Arrangements of Ionic Charge in Zeolite Frameworks Conferred by Specific Aluminum Distributions Preferentially Stabilize Alkanol Dehydration Transition States. Angewandte Chemie - International Edition, 2020, 59, 18686-18694.	7.2	29
11	Oxophilicity Drives Oxygen Transfer at a Palladium–Silver Interface for Increased CO Oxidation Activity. ACS Catalysis, 2020, 10, 13878-13889.	5.5	7
12	Rigid Arrangements of Ionic Charge in Zeolite Frameworks Conferred by Specific Aluminum Distributions Preferentially Stabilize Alkanol Dehydration Transition States. Angewandte Chemie, 2020, 132, 18845-18853.	1.6	22
13	Highly Selective Cross-Etherification of 5-Hydroxymethylfurfural with Ethanol. ACS Catalysis, 2020, 10, 6771-6785.	5.5	40
14	Mechanism and Effects of Coverage and Particle Morphology on Rh-Catalyzed NO–H ₂ Reactions. Journal of Physical Chemistry C, 2020, 124, 13291-13303.	1.5	10
15	Contrasting Arene, Alkene, Diene, and Formaldehyde Hydrogenation in H-ZSM-5, H-SSZ-13, and H-SAPO-34 Frameworks during MTO. ACS Catalysis, 2020, 10, 4593-4607.	5.5	38
16	Impact of Metal and Heteroatom Identities in the Hydrogenolysis of C–X Bonds (X = C, N, O, S, and Cl). ACS Catalysis, 2020, 10, 5086-5100.	5.5	21
17	In Situ Methods for Identifying Reactive Surface Intermediates during Hydrogenolysis Reactions: C–O Bond Cleavage on Nanoparticles of Nickel and Nickel Phosphides. Journal of the American Chemical Society, 2019, 141, 16671-16684.	6.6	30
18	Hydrogen Chemisorption Isotherms on Platinum Particles at Catalytic Temperatures: Langmuir and Two-Dimensional Gas Models Revisited. Journal of Physical Chemistry C, 2019, 123, 8447-8462.	1.5	28

DAVID D HIBBITTS

#	Article	IF	CITATIONS
19	Comparing Rate and Mechanism of Ethane Hydrogenolysis on Transition-Metal Catalysts. Journal of Physical Chemistry C, 2019, 123, 5421-5432.	1.5	31
20	Mechanism and Kinetics of Methylating C ₆ –C ₁₂ Methylbenzenes with Methanol and Dimethyl Ether in H-MFI Zeolites. ACS Catalysis, 2019, 9, 6444-6460.	5.5	45
21	Restructuring of MFI Framework Zeolite Models and Their Associated Artifacts in Density Functional Theory Calculations. Journal of Physical Chemistry C, 2019, 123, 6572-6585.	1.5	21
22	Mechanistic origins of the high-pressure inhibition of methanol dehydration rates in small-pore acidic zeolites. Journal of Catalysis, 2019, 380, 161-177.	3.1	40
23	Supraâ€monolayer coverages on small metal clusters and their effects on H ₂ chemisorption particle size estimates. AICHE Journal, 2018, 64, 3109-3120.	1.8	24
24	Dominant Role of Entropy in Stabilizing Sugar Isomerization Transition States within Hydrophobic Zeolite Pores. Journal of the American Chemical Society, 2018, 140, 14244-14266.	6.6	83
25	Effects of Catalyst Model and High Adsorbate Coverages in ab Initio Studies of Alkane Hydrogenolysis. ACS Catalysis, 2018, 8, 6375-6387.	5.5	21
26	Mechanisms and Active Sites for C–O Bond Rupture within 2-Methyltetrahydrofuran over Ni, Ni ₁₂ P ₅ , and Ni ₂ P Catalysts. ACS Catalysis, 2018, 8, 7141-7157.	5.5	29
27	Tuning BrĄ̃nsted Acid Strength by Altering Site Proximity in CHA Framework Zeolites. ACS Catalysis, 2018, 8, 7842-7860.	5.5	41
28	Dense CO Adlayers as Enablers of CO Hydrogenation Turnovers on Ru Surfaces. Journal of the American Chemical Society, 2017, 139, 11789-11802.	6.6	54
29	Interfacial charge distributions in carbon-supported palladium catalysts. Nature Communications, 2017, 8, 340.	5.8	145
30	Theoretical insights into the sites and mechanisms for base catalyzed esterification and aldol condensation reactions over Cu. Faraday Discussions, 2017, 197, 59-86.	1.6	23
31	Promotional effects of chemisorbed oxygen and hydroxide in the activation of C–H and O–H bonds over transition metal surfaces. Surface Science, 2016, 650, 210-220.	0.8	57
32	Effects of Chain Length on the Mechanism and Rates of Metal-Catalyzed Hydrogenolysis of <i>n</i> -Alkanes. Journal of Physical Chemistry C, 2016, 120, 8125-8138.	1.5	49
33	Preferential activation of CO near hydrocarbon chains during Fischer–Tropsch synthesis on Ru. Journal of Catalysis, 2016, 337, 91-101.	3.1	54
34	Role of Branching on the Rate and Mechanism of C–C Cleavage in Alkanes on Metal Surfaces. ACS Catalysis, 2016, 6, 469-482.	5.5	40
35	Prevalence of Bimolecular Routes in the Activation of Diatomic Molecules with Strong Chemical Bonds (O2, NO, CO, N2) on Catalytic Surfaces. Accounts of Chemical Research, 2015, 48, 1254-1262.	7.6	53
36	Kinetic and Mechanistic Assessment of Alkanol/Alkanal Decarbonylation and Deoxygenation Pathways on Metal Catalysts. Journal of the American Chemical Society, 2015, 137, 11984-11995.	6.6	55

DAVID D HIBBITTS

#	Article	IF	CITATIONS
37	Theoretical and kinetic assessment of the mechanism of ethane hydrogenolysis on metal surfaces saturated with chemisorbed hydrogen. Journal of Catalysis, 2014, 311, 350-356.	3.1	55
38	Acid strength and bifunctional catalytic behavior of alloys comprised of noble metals and oxophilic metal promoters. Journal of Catalysis, 2014, 315, 48-58.	3.1	39
39	Metal-Catalyzed C–C Bond Cleavage in Alkanes: Effects of Methyl Substitution on Transition-State Structures and Stability. Journal of the American Chemical Society, 2014, 136, 9664-9676.	6.6	87
40	Catalytic NO activation and NOâ \in "H 2 reaction pathways. Journal of Catalysis, 2014, 319, 95-109.	3.1	31
41	Electrocatalysis: A direct alcohol fuel cell and surface science perspective. Catalysis Today, 2013, 202, 197-209.	2.2	130
42	Influence of oxygen and pH on the selective oxidation of ethanol on Pd catalysts. Journal of Catalysis, 2013, 299, 261-271.	3.1	63
43	Mechanistic Role of Water on the Rate and Selectivity of Fischer–Tropsch Synthesis on Ruthenium Catalysts. Angewandte Chemie - International Edition, 2013, 52, 12273-12278.	7.2	138
44	Selective Hydrogenolysis of Polyols and Cyclic Ethers over Bifunctional Surface Sites on Rhodium–Rhenium Catalysts. Journal of the American Chemical Society, 2011, 133, 12675-12689.	6.6	439
45	Reactivity of the Gold/Water Interface During Selective Oxidation Catalysis. Science, 2010, 330, 74-78.	6.0	888